Traffic Volume Detection Using Infrastructure-based LiDAR under Different Level of Service Conditions

Junxuan Zhao[1]

Hao Xu[2]

Yibin Zhang[3]

Yuan Tian[4]

Hongchao Liu[5]

ABSTRACT

Light detection and ranging (LiDAR) technology is a key component of an autonomous vehicle's sensing system. It also has the potential to be used at roadside as a major infrastructure-based detection for connected vehicle-infrastructure systems, as well as for the general purpose of traffic detection. This paper presents the results of a sponsored research on using LiDAR to detect traffic volume. Like other video-based sensors, occlusion is a major cause of error for traffic volume detection. In this study, a method for automatic identifying and classification of LiDAR specific occlusion was first developed based on the inherent characteristics of LiDAR sensors, such as the number of laser beams, vertical field of view (FOV) and degree of resolution, and rotation frequency etc.; Then, the model was implemented in traffic simulation to generate occlusion rates

---

[1]Postdoctoral Researcher, Dept. of Civil, Environmental, and Construction Engineering, Texas Tech Univ., Lubbock, TX 79409. E-mail: junxuan.zhao@ttu.edu
[2]Associate Professor, Dept. of Civil and Environmental Engineering, Univ. of Nevada Reno, Reno, NV 89557. E-mail: haox@unr.edu
[3]Ph.D. Student, Dept. of Civil, Environmental, and Construction Engineering, Texas Tech Univ., Lubbock, TX 79409. E-mail: yibin.zhang@ttu.edu
[4]Ph.D. Student, Dept. of Civil and Environmental Engineering, Univ. of Nevada Reno, Reno, NV 89557. E-mail: yuantian@nevada.unr.edu
[5]Professor, Dept. of Civil, Environmental, and Construction Engineering, Texas Tech Univ., Lubbock, TX 79409 (corresponding author). E-mail: hongchao.liu@ttu.edu

under various level of service (LOS A to E) and different truck compositions (5%-30%); Lastly, data collected from two testbeds were used to examine the accuracy of the methodological approach and the simulation results. The testbeds include a freeway segment on I-80 and a major arterial of US 395 & North McCarran Boulevard in the Washoe County of Nevada. The result shows that using two 32-laser LiDAR sensors, an average of 95% detection accuracy could be achieved for the worst scenario of LOS E with 30% trucks.

***Keywords*:** Infrastructure-based LiDAR, Traffic volume, Level of Service, Occlusion.

Introduction

From inductive loop to video camera, traffic detection technologies continue to evolve and escalate (Guo et al., 2008; Fulari et al. 2017; He et al. 2019). Originally used for aerial survey, healthcare, geoscience and more, LiDAR is becoming ever more popular in the transportation industry after being utilized in autonomous vehicles as a key sensing technology for collision avoidance, obstacle detection, and autonomous cruise control (Liu et al. 2014; Wang et al. 2017; Kukkala et al. 2018; Zeng et al. 2018). LiDAR is a typical non-contact sensing technology which measures distance to an object by illuminating the target with pulsed laser light and analyzing the reflected pulses. It provides 3-dimensional (3D) image based on the differences in laser return times and wavelengths. In addition to its speed and accuracy, LiDAR sensors can provide 360-degree surveillance in real-time and are thus ideal for real-time and trajectory-level traffic detection.

The research team has conducted a wealth of studies to investigate the feasibility of using LiDAR sensor at the roadside as a major solution for real-time traffic detection (Wu et al. 2020a; Wu et al. 2020b). This research was developed based on the results of two previous studies on how to process roadside LiDAR data for traffic and pedestrian detection (Zhao et al. 2019b), and how to install LiDAR sensor at roadside for best performance (Zhao et al. 2020). A major objective of this study is to investigate the accuracy of using LiDAR to detect traffic volume under various traffic conditions. The research mainly involves developing a method for automatic identifying and classification of LiDAR specific occlusion and a combined simulation and experimental approach for systematic evaluation. The analytical method was developed based on the inherent characteristics of LiDAR sensors, such as the number of laser beams, vertical field of view (FOV) and degree of resolution, and rotation frequency. Traffic simulation was used to get occlusion rates by using the analytical method under various level of service conditions (LOS A to E) and different truck compositions (5%-30%); For experimental study, two testbeds were constructed on a segment of I-80 and a major arterial of US 395 & North McCarran Boulevard in the Washoe County of Nevada.

Occlusion is a major cause of error for image-based detection. For practitioners, it is important to understand the expected occlusion rates and the resulted detection accuracy under various traffic conditions before field implementation of LiDAR sensors. Occlusion exists at different levels and can be mainly divided into three categories: partial occlusion, full occlusion, and non-occlusion. Among them, full occlusion certainly has the worst impact on traffic volume detection because the occluded vehicle cannot be detected and thus will be missing in the counts. Previous studies on occlusion have been primarily focused on how to identify the occurrence of occlusion, determine the degree of occlusion, and develop methods to mitigate the impacts of occlusion in vehicle detection (Wang et al. 2016; Phan et al. 2017), classification (Castillo et al. 2017; Chang et al. 2018; Moutakki et al. 2018), counting (Moutakki et al. 2017; Velazquez-Pupo et al. 2018) and tracking (Veeraraghavan et al. 2003; Joshi et al. 2019). Studies similar to this research that develops corresponding relationship between occlusion rates and detection accuracy covering all LOS conditions except LOS F have not been found in the literature.

As video cameras have been widely applied in traffic detection (Zhang and Du 2020; Zhuang et al. 2020), it is necessary to give a brief review about its performance. According to the benchmark before 2012 (Dollár et al. 2009; Dollár et al. 2011; Geiger et al. 2012), the accuracy of using video cameras to detect partially occluded vehicles, heavily occluded vehicles, and occluded pedestrians is about 90%, 80%, 65%~75%, respectively. The recent KITTI Vision Benchmark (Gilroy et al. 2019) shows that the detection accuracy has been improved to vehicle (partial occlusion 90%; heavy occlusion 77%~87%), pedestrian (partial occlusion 71%~77%; heavy occlusion 66%~74%), and cyclists (partial occlusion 72%~76%; heavy occlusion 65%). One major weakness of video detection is night-time detection and the impact from inclement weather such as heavy winds, rain, and snow (Mukhtar et al. 2015). Additionally, large vehicles may project their images into adjacent lanes, resulting in overcount and false average speeds (Klein et al. 2006). In comparison, LiDAR sensors are more resistant to such weather conditions. In terms of accuracy, this research shows that using two 32-laser LiDAR sensors, an average of 95% detection accuracy could be achieved for the worst scenario of LOS E with 30% trucks.

LiDAR Sensors and Operational Principle

LiDAR uses eye-safe laser beams to create high-precision 3D point cloud representation and one data frame is generated after the sensor completes a 360-degree scan. The location of each recorded data point can be described in two coordinate systems, namely, the Cartesian coordinate system with (X, Y, Z) and the spherical coordinate system with (R, ω, α). They can be converted to each other using coordinate transformations (Velodyne 2016).

LiDAR emits pulsed light waves and uses the time a pulse takes to return to calculate the distance it travels, our study shows that when installed at roadside, it outperforms many other detection means in measuring speed, location and trajectory of all road users including pedestrians in real-time (Wu et al. 2018; Zhao et al. 2019a). A LiDAR sensor is usually securely mounted within a compact, weather-resistant housing and each laser beam rotates 360-degree along the sensor's central axis with a fixed elevation angle to form a conical surface for scan. Also, a laser beam travels along a straight line with a certain direction but cannot continue to propagate after shooting an object (cause of occlusion). In practice, these inherent properties need to be investigated to guide installation. This research directly uses the findings from a previous study on how to install LiDAR sensors in the field, the authors refer the interested readers to Zhao et al. (2020).

Selection of LiDAR sensors should be based upon a combined consideration of cost and performance, our studies have found 16- and 32-beam LiDAR sensors are most cost-effective for roadside application (Zhao et al. 2020). In this study we used the Puck (VLP-16) (Velodyne 2016) and the Ultra Puck (VLP-32C) (Velodyne 2018) LiDAR sensors from Velodyne LiDAR Inc. The entry-level Puck sensor provides 16 laser beams and a FOV from −15° to +15° with 2° resolution. The Ultra Puck sensor provides 32 laser beams with a FOV from −25° to +15°, in which the vertical resolution of the laser beams is non-linear (0.33° for −4° to +1.33° FOV, others are non-linear). The rotation frequency of both types of LiDAR sensors can be customized from 5Hz to 20Hz.

Method for Classification and Evaluation of Vehicle Occlusion in Infrastructure-based LiDAR Detection

In this study, three occlusion levels were examined:

1) Fully detectable objects: the objects can be detected completely (No occlusion).

2) Partially detectable objects: the objects can be detected partially (Partial occlusion).

3) Undetectable objects: the objects cannot be detected (Full occlusion).

For illustrative purpose, Fig. 1 demonstrates the above three occlusion scenarios, where vehicle #1 is partially occluded by vehicle #3, vehicle #6 is fully occluded by vehicle #5, and vehicles #2, #3, #4, #5, #7 are not occluded and fully detectable.

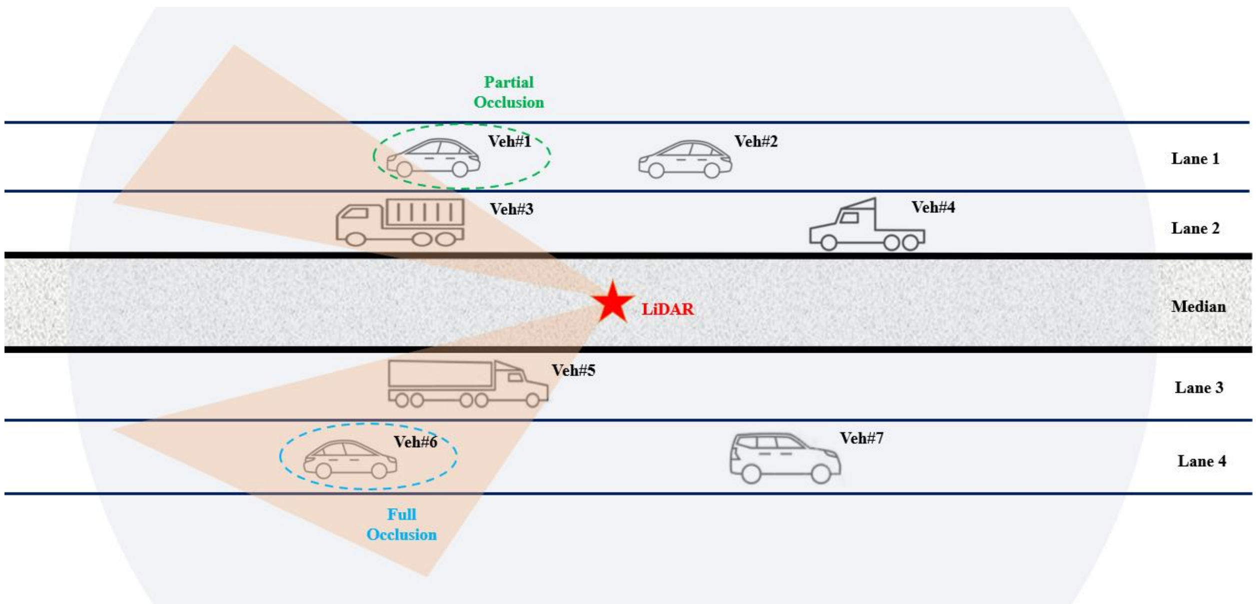

Fig. 1. Three occlusion levels of vehicles.

Classification of Vehicle Occlusion Types Using Roadside LiDAR Data

For a specific LiDAR sensor installed at roadside, the horizontal and vertical direction of each laser beam is known at a specific moment, which means that for a specific traffic scene at a certain moment, it is certain whether a laser beam can reach the surface of a vehicle. If so, the exact location of the reflection point can also be determined. During each 360-degree scan (one data frame), each vehicle's ID and the 3D distance between the LiDAR sensor and the reflection point are critical for determination of occlusion types. To effectively process this information, the authors developed a 2D table/matrix structure H (defined by Eq. (1)) based on the configuration of the applied LiDAR sensors, with each row of the table representing each elevation angle/channel of the laser beams, and each column of the table representing each azimuth interval of the laser beams during 0-degree to 360-degree scan. The contents of the table are the vehicle ID(s) with the corresponding 3D distance(s) (defined by Eq. (2)). This way, vehicles' information which are measured by the same laser beam at the same azimuth interval is recorded in the same cell of the 2D table.

$$\mathrm{H}_{\mathrm{W\times L}} = \begin{bmatrix} \mathrm{Q}_{(1,1)} & \mathrm{Q}_{(1,2)} & \cdots & \mathrm{Q}_{(1,n)} & \cdots & \mathrm{Q}_{(1,L)} \\ \mathrm{Q}_{(2,1)} & \mathrm{Q}_{(2,2)} & \cdots & \mathrm{Q}_{(2,n)} & \cdots & \mathrm{Q}_{(2,L)} \\ \vdots & \vdots & \vdots & \vdots & \vdots & \vdots \\ \mathrm{Q}_{(m,1)} & \mathrm{Q}_{(m,2)} & \cdots & \mathrm{Q}_{(m,n)} & \cdots & \mathrm{Q}_{(m,L)} \\ \vdots & \vdots & \vdots & \vdots & \vdots & \vdots \\ \mathrm{Q}_{(W,1)} & \mathrm{Q}_{(W,2)} & \cdots & \mathrm{Q}_{(W,n)} & \cdots & \mathrm{Q}_{(W,L)} \end{bmatrix} \quad (1)$$

$$\mathrm{Q}_{(\mathrm{m,n})} = \begin{bmatrix} vehID(1) & distance\ (1) \\ vehID(2) & distance\ (2) \\ \vdots & \vdots \\ vehID(s) & distance\ (s) \end{bmatrix} (m = 1,2, \ldots W; n = 1,2, \ldots, L) \quad (2)$$

Where W is the total number of laser IDs and L is the total number of azimuth intervals within a 360-degree scan; $Q_{(m,n)}$ includes both vehicle's ID and the distance information of s vehicles that are detected by the laser m at the azimuth angle n.

To classify detected vehicles in a data frame into different occlusion categories, a judgment is made based on the information stored in the 2D table of that data frame. If each vehicle is considered individually, the number of data points collected from each vehicle during a 360-degree scan can be calculated by counting the number of times (M) the vehicle's ID appeared in the 2D table. If more than one vehicle's information are saved in the same cell, the first vehicle occludes all other vehicles (vehicles are sorted by distance from near to far) because a specific laser beam at a specific azimuth cannot be used again after it shot the first vehicle. This way, the number of times (N) each occluded vehicle ID appeared in the 2D table can also be obtained. Comparing M

and N, the vehicle occlusion level can be determined: full detection ($M > N = 0$), partial detection ($M > N > 0$), and non-detection ($M = N$). When two LiDAR sensors are used, detection of each vehicle from two sensors is independent. If a vehicle can be fully detected by at least one sensor, the vehicle is labeled as full detection; if a vehicle cannot be detected by any sensor, the vehicle is labeled as non-detection; for other detection combinations, the vehicle is labeled as partial detection. The proposed classification process is illustrated in Fig. 2.

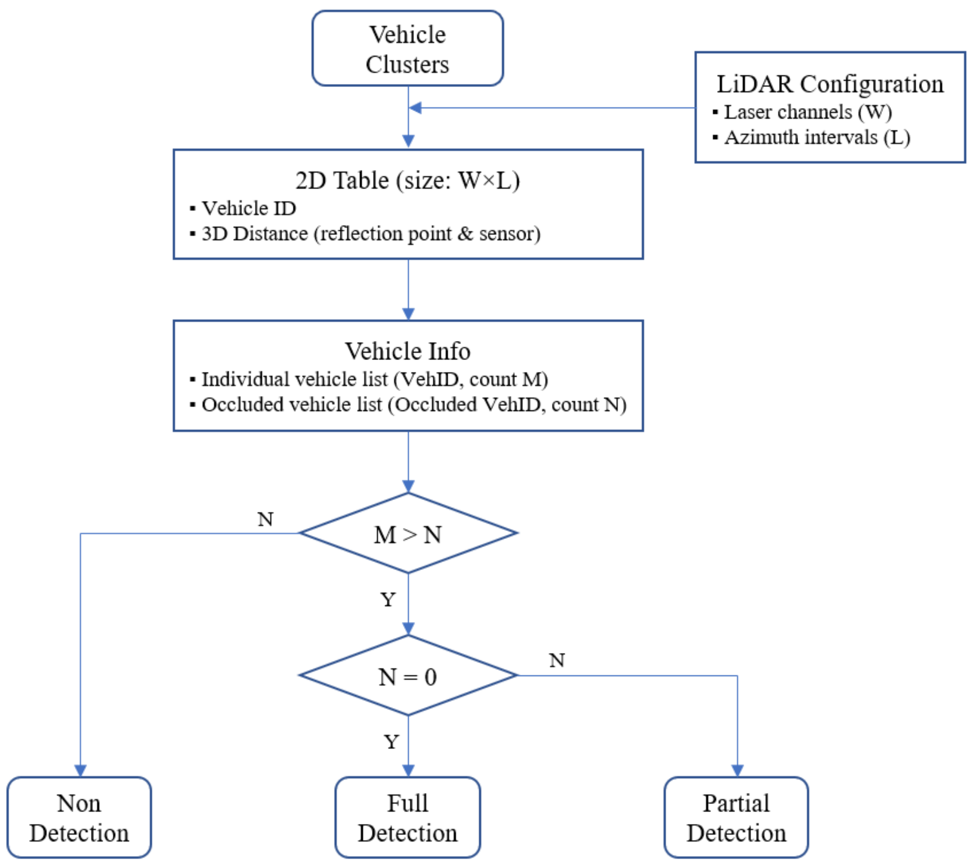

Fig. 2. Flowchart of vehicle occlusion classification.

Evaluation Indices of Vehicle Occlusion

Assuming T continuous frames are collected, in the i^{th} frame ($i = 1,2,3, \dots, T$), a total of K_i vehicles are detected, including a_i fully detectable vehicles, b_i partially detectable vehicles, and

c_i undetectable vehicles. To quantitatively evaluate the level of vehicle occlusion, the following indices are defined:

1) $Fully\ Detectable\ Rate = \frac{\sum_{i=1}^{T} a_i}{\sum_{i=1}^{T} K_i}$ (3)

2) $Partially\ Detectable\ Rate = \frac{\sum_{i=1}^{T} b_i}{\sum_{i=1}^{T} K_i}$ (4)

3) $Undetectable\ Rate = \frac{\sum_{i=1}^{T} c_i}{\sum_{i=1}^{T} K_i}$ (5)

Assuming the maximum number of consecutive undetectable frames is P and the total number of undetectable vehicles that satisfies this criterion is D_P, the percentage of undetectable vehicles is:

4) $Percentage\ of\ Undetectable\ Vehicles(\text{consecutive}\ for\ P\ frames) = \frac{D_P}{\sum_{i=1}^{T} K_i}$ (6)

Evaluation of Occlusion Influence on Vehicle Detection Using simulation Data

To develop different LOS environments with various truck compositions, simulation was used, in which the proposed method was implemented to get occlusion rates under various level of service (LOS A to E) and different truck compositions (5%-30%).

Simulation Scenarios

A total of 30 traffic scenarios along an urban freeway segment was simulated in PTV Vissim to evaluate the impact of occlusion on vehicle detection (as shown in Fig. 3). The details of the developed simulation environment are introduced below:

1) Urban freeway segment

   1000 m length; 4 lanes (2 lanes in each direction) with 3.66m width; median with 17.6m width; 2.5 m right-side lateral clearance and 2 ramps per mile.

2) FFS (free-flow speed) = 31.29 m/s.

3) PHF (peak hour factor) = 0.95; f_p(driver population adjustment factor) = 1.0; E_T (passenger-car equivalents) = 1.5 (type of terrain: level).

4) LiDAR sensor: Puck (VLP-16) and Ultra Puck (VLP-32C), 10Hz rotation frequency.
   Installation: LiDAR 1 is horizontally installed at the median (500m, 0m, 2.4m) location.
   LiDAR 2 is horizontally installed at the median (550m, 0m, 2.4m) location.
   (Zhao et al. 2020)

5) Region of Interest (ROI): [400m, 600m].

6) Level of Service (LOS): A, B, C, D, E.

7) Vehicle size: Passenger car (L = 4.5m, W = 1.8m, H = 1.6m).
   Truck (L = 16.2m, W = 2.6m, H = 2.6m).
   (Hancock and Wright, 2013)

8) Percentage of trucks: 5%, 10%, 15%, 20%, 25%, 30%.

Traffic volumes were generated based on the above settings.

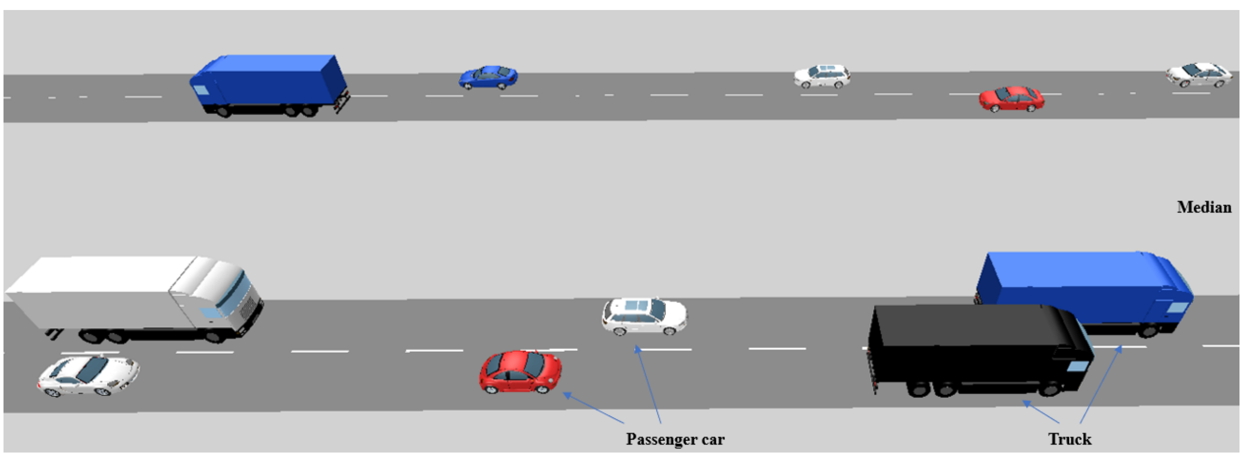

Fig. 3. Simulation of traffic flow.

Summary of Simulation Results

Both single and paired LiDAR sensor application were used in simulation and the detection rate was classified based on fully detectable, partially detectable, and undetectable. Additionally, the percentage of undetectable vehicles was evaluated in two consecutive time intervals – undetectable for at least 0.5 seconds and undetectable for at least 1.0 second. Results are summarized in Table 1(a) (one 16-laser LiDAR sensor application), Table 1(b) (two 16-laser LiDAR sensor application), and Table 2(a) (one 32-laser LiDAR sensor application), and Table 2(b) (two 32-laser LiDAR sensor application).

The results show that:

1) Using the “undetectable rate” as an indicator, an average accuracy of 95% could be achieved for the worst scenario of LOS E with 30% trucks if two LiDAR sensors are applied, therefore, a pair of 16-laser LiDAR sensors should be recommended considering the cost.
2) Undetectable rate increases with the increase of both LOS level and the percentage of trucks and using one single higher-end 32-laser sensor does not help much, instead, a pair of lower cost 16-laser sensors should be used.
3) There seems to be a large leap in undetectable rate when the truck percentage increases from 25% to 30%.
4) If the truck volume is lower than 25%, one single 32-laser LiDAR sensor can be recommended for an expected accuracy of 92-94%.

Validation Using Field Data

With coordinated efforts from the Nevada Department of Transportation, the City of Reno and the Regional Transportation Commission (RTC), two test sites were developed, which include a segment of I-80 (39.51°N, −119.94°W) and a segment of US395 & North McCarran Boulevard (39.55N, −119.79°W).

Fig. 4. Data collection sites.

For both sites, one single 32-channel LiDAR sensor (VLP-32C, 10Hz) was used in consideration of the cost and truck volume. At the I-80 site, the sensor was installed at the median area, at the US395 site, the sensor was installed at the southbound on-ramp area as shown in Fig. 4. At the I-80 site, data collected on August 15th, 2019 from 7 am to 8 am were used for validation, at the US395 site, data collected on August 28th, 2019, also from the morning peak of 7 am to 8 am were used. For each dataset, the one-hour volume was divided into twelve 5-minute intervals. As can be seen in Table 3 and Table 4, data from the I-80 site captured a dynamic truck composition of 8.49% to 23.30% while the LOS remained at LOS B. At the US395 site, LOS varied in the range of LOS C to LOS E while the percentage of trucks was constantly lower than 6%. Combined, data collected from two test sites covered a LOS range of B to E and a truck composition range of 2.79% to 23.30%. Although it is unfortunate some of the scenarios in simulation with both high LOS and heavy truck volume were not captured from the two sites, the data covered most of the scenarios and were sufficient for the purpose of validation.

Using the proposed automatic occlusion detection algorithm and the partially detectable rate as the parameter, comparison analysis was conducted. The reason why the partially detectable rate was selected should be straightforward, as the number of fully undetectable vehicles could not be verified without the ground truth traffic counts. As shown in Table 3 and Table 4, comparing the experimental results with the corresponding simulation results under the same LOS level and similar truck percentage conditions, the average offsets of partially detectable rates for the two sites are 0.92% and 0.62%, respectively, which strongly support the simulation results.

Conclusion

This paper presents part of a continuous study on the feasibility of using LiDAR as a major infrastructure-based traffic detection, with focus on the accuracy of traffic volume detection and how traffic condition and truck composition affect the results. A method for automatic identification of LiDAR-based occlusion was developed, which was implemented in traffic simulation with a total of 30 simulation scenarios covering the Level of Services A to E and the truck percentage from 5% to 30%. The simulation results were examined against field data collected from two test sites. The study was conducted based on two-lane (per direction) highways owing to the interest of the sponsoring agency, but the proposed method is applicable to other scenarios because it was developed based on the inherent features of LiDAR sensors. In summary, one 32-laser LiDAR sensor is recommended if the truck percentage is lower than 25%, otherwise, a pair of 16-laser sensors should be considered for two-lane surveillance. Additionally, the information provided in Table 1 and Table 2 can help transportation agencies to make informed decisions when considering LiDAR as their choice of sensing technology in the field.

Limitations of the study include missing LOS F in the analysis, due in part to the fact that traffic is highly unstable at LOS F and in part to the lack of necessary test sites, and missing scenarios with higher truck volume, which is inherent to the traffic condition at the test sites.

Data Availability Statement

Some or all data, models, or code that support the findings of this study are available from the corresponding author upon reasonable request.

Acknowledgement

This work was supported by the Nevada Department of Transportation (NDOT) [Grant No. P224-14-803/TO #13]. The authors gratefully acknowledge this financial support. This research was also supported by engineers with the Nevada Department of Transportation, the Regional Transportation Commission of Washoe County, Nevada, and the City of Reno.

References

Castillo, R. D. M., M. M. B. Tejada, M. O. Cordel, A. F. B. Laguna, and J. P. Ilao. 2017. "Vsion: Vehicle occlusion handling for traffic monitoring." In *Proc., Int. Conf. on Video and Image Processing*, 167-171. Jurong West, Singapore: Nanyang Technol. Univ. https://doi.org/10.1145/3177404.3177431

Chang, J., L. Wang, G. Meng, S. Xiang, and C. Pan. 2018. "Vision-based occlusion handling and vehicle classification for traffic surveillance systems." *IEEE Intell. Transp. Syst. Mag.* 10(2): 80-92. https://doi.org/10.1109/MITS.2018.2806619

Dollár, P., C. Wojek, B. Schiele, and P. Perona. 2009. "Pedestrian detection: A benchmark." In *Proc., IEEE Conf. on Computer Vision and Pattern Recognition*, 304-311. Miami, FL, USA: IEEE Computer Society. https://doi.org/10.1109/CVPR.2009.5206631

Dollár, P., C. Wojek, B. Schiele, and P. Perona. 2011. "Pedestrian detection: An evaluation of the state of the art." *IEEE Trans. Pattern Anal. Mach. Intell.* 34(4): 743-761. https://doi.org/10.1109/TPAMI.2011.155

Fulari, S., L. Vanajakshi, and S. C. Subramanian. 2017. “Artificial neural network–based traffic state estimation using erroneous automated sensor data.” *J. Transp. Eng. Part A: Syst.* 143(8): 05017003. https://doi.org/10.1061/JTEPBS.0000058

Geiger, A., P. Lenz, P., and R. Urtasun. 2012. “Are we ready for autonomous driving? The KITTI vision benchmark suite.” In *Proc., IEEE Conf. on Computer Vision and Pattern Recognition*, 3354-3361. Providence, RI, USA. https://doi.org/10.1109/CVPR.2012.6248074

Gilroy, S., E. Jones, and M. Glavin. 2019. “Overcoming Occlusion in the Automotive Environment-A Review.” *IEEE Trans. Intell. Transp. Syst.* https://doi.org/10.1109/TITS.2019.2956813

Guo, J., J. Xia, and B. L. Smith. 2008. *Investigation of speed estimation using single loop detectors*. Univ. of Virginia. Center for Transportation Studies. https://rosap.ntl.bts.gov/view/dot/16553

Hancock, M. W., and B. Wright. 2013. *A policy on geometric design of highways and streets*. American Association of State Highway and Transportation Officials: Washington, DC, USA.

He, Z., J. Hu, B. B. Park, and M. W. Levin. 2019. “Vehicle sensor data-based transportation research: Modeling, analysis, and management.” *J. Intell. Transp. Syst.* 23: 99-102. https://doi.org/10.1080/15472450.2019.1586335

Joshi, R. C., A. G. Singh, M. Joshi, and S. Mathur. 2019. “A Low Cost and Computationally Efficient Approach for Occlusion Handling in Video Surveillance Systems.” *Int. J. Interact. Multi. Artif. Intell.* 5(7): 28-38. https://doi.org/10.9781/ijimai.2019.01.001

Klein, L. A., M. K. Mills, and D. R. Gibson. 2006. *Traffic detector handbook: Volume I* (No. FHWA-HRT-06-108). Turner-Fairbank Highway Research Center.

Kukkala, V. K., J. Tunnell, S. Pasricha, and T. Bradley. 2018. “Advanced driver-assistance systems: A path toward autonomous vehicles.” *IEEE Consum. Electron. Mag.* 7(5): 18-25. https://doi.org/10.1109/MCE.2018.2828440

Liu, J., P. Jayakumar, J. L. Stein, and T. Ersal. 2014. “A multi-stage optimization formulation for MPC-based obstacle avoidance in autonomous vehicles using a LIDAR sensor.” In *Proc., Dyn. Syst. Control Conf.*, 46193(V002T30A006). San Antonio, TX, USA: ASME. https://doi.org/10.1115/DSCC2014-6269

Moutakki, Z., I. M. Ouloul, K. Afdel, and A. Amghar. 2017. “Real-time video surveillance system for traffic management with background subtraction using codebook model and occlusion handling.” *Trans. Telecomm. J.* 18(4): 297-306. https://doi.org/10.1515/ttj-2017-0027

Moutakki, Z., I. M. Ouloul, K. Afdel, and A. Amghar. 2018. “Real-time system based on feature extraction for vehicle detection and classification.” *Trans. Telecomm. J. 19*(2): 93-102. https://doi.org/10.2478/ttj-2018-0008

Mukhtar, A., L. Xia, and T. B. Tang. 2015. “Vehicle detection techniques for collision avoidance systems: A review.” *IEEE Trans. Intell. Transp. Syst.* 16(5): 2318-2338. https://doi.org/10.1109/TITS.2015.2409109

Phan, H. N., L. H. Pham, D. N. N. Tran, and S. V. U. Ha. 2017. “Occlusion vehicle detection algorithm in crowded scene for traffic surveillance system.” In *Proc., Int. Conf. on Syst. Sci. Eng.*, 215-220. Ho Chi Minh City, Vietnam: IEEE. https://doi.org/10.1109/ICSSE.2017.8030868

Veeraraghavan, H., O. Masoud, and N. P. Papanikolopoulos. 2003. “Computer vision algorithms for intersection monitoring.” *IEEE Trans. Intell. Transp. Syst.* 4(2): 78-89. https://doi.org/10.1109/TITS.2003.821212

Velazquez-Pupo, R., A. Sierra-Romero, D. Torres-Roman, Y. V. Shkvarko, J. Santiago-Paz, D. Gómez-Gutiérrez, and M. Romero-Delgado. 2018. “Vehicle detection with occlusion handling, tracking, and OC-SVM classification: A high performance vision-based system.” *Sensors*, 18(2): 374. https://doi.org/10.3390/s18020374

Velodyne. 2016. *VLP-16 manual: User’s manual and programming guide*. Velodyne LiDAR. Inc.

Velodyne. 2018. *VLP-32C user manual*. Velodyne LiDAR.Inc.

Wang, H., Y. Cai, X. Chen, and L. Chen. 2016. “Occluded vehicle detection with local connected deep model.” *Multimed. Tools. Appl.* 75(15): 9277-9293. https://doi.org/ 10.1007/s11042-015-3141-0

Wang, H., B. Wang, B. Liu, X. Meng, and G. Yang. 2017. “Pedestrian recognition and tracking using 3D LiDAR for autonomous vehicle.” *Rob. Auton. Syst.* 88: 71-78. https://doi.org/10.1016/j.robot.2016.11.014

Wu, J., H. Xu, Y. Zhang, Y. Tian, and X. Song. 2020a. “Real-time queue length detection with roadside LiDAR data.” *Sensors*, 20(8): 2342. https://doi.org/10.3390/s20082342

Wu, J., H. Xu, J. Zheng, and J. Zhao. 2020b. “Automatic vehicle detection with roadside LiDAR data under rainy and snowy conditions.” *IEEE Intell. Transp. Syst. Mag.* https://doi.org/10.1109/MITS.2019.2926362

Wu, J., H. Xu, Y. Zheng, and Z. Tian. 2018. “A novel method of vehicle-pedestrian near-crash identification with roadside LiDAR data.” *Accid. Anal. Prev.* 121: 238-249. https://doi.org/10.1016/j.aap.2018.09.001

Zeng, Y., Y. Hu, S. Liu, J. Ye, Y. Han, X. Li, and N. Sun. 2018. “Rt3d: Real-time 3-d vehicle detection in lidar point cloud for autonomous driving.” *IEEE Robot. Autom. Lett.* 3(4): 3434-3440. https://doi.org/10.1109/LRA.2018.2852843

Zhao, J., Y. Li, H. Xu, and H. Liu. 2019a. “Probabilistic prediction of pedestrian crossing intention using roadside LiDAR data.” *IEEE Access*, 7: 93781-93790. https://doi.org/ 10.1109/ACCESS.2019.2927889

Zhao, J., H. Xu, H. Liu, J. Wu, Y. Zheng, and D. Wu. 2019b. “Detection and tracking of pedestrians and vehicles using roadside LiDAR sensors.” *Transp. Res. Part C: Emerging. Technol. 100*: 68-87. https://doi.org/10.1016/j.trc.2019.01.007

Zhao, J., H. Xu, Y. Tian, and H. Liu. 2020. “Towards application of light detection and ranging sensor to traffic detection: an investigation of its built-in features and installation techniques.” *J. Intell. Transp. Syst.*1-22. https://doi.org/10.1080/15472450.2020.1807346

Zhang, C., and B. Du. 2020. "Image-Based Approach for Parking-Spot Detection with Occlusion Handling." *J. Transp. Eng. Part A: Syst.* 146(9): 04020098. https://doi.org/10.1061/JTEPBS.0000420

Zhuang, Y., R. Ke, and Y. Wang. 2020. "Edge-Based Traffic Flow Data Collection Method Using Onboard Monocular Camera." *J. Transp. Eng. Part A: Syst.* 146(9): 04020096. https://doi.org/10.1061/JTEPBS.0000416